The Addition Effects of Methyl Halides on Ethane Ignition Behind Reflected Shock Waves

Kazuo TAKAHASHI, Tadaaki INOMATA,* Takao MORIWAKI, and Satiko OKAZAKI
Department of Chemistry, Faculty of Science and Technology, Sophia University,
7-1 Kioi-cho, Chiyoda-ku, Tokyo 102
(Received November 29, 1988)

Ignition delay times were measured in C_2H_6–O_2–CH_3X(X:Cl, Br or I) mixtures highly diluted with argon behind reflected shock waves. The measurements covered a temperature range of 1200—1900 K and the pressure range of 1.4—2.9 atm. The times were longer than those without CH_3X, indicating that CH_3X inhibits ethane ignition. This was contrary to the previous results which showed that CH_3X promoted methane ignition. To clarify the addition effects of CH_3X from the viewpoint of the reaction mechanism, computational analyses were performed in C_2H_6–O_2–CH_3Br and CH_4–O_2–CH_3Br mixtures. The analytical results showed that different chain cycles for Br-containing species were formed in the two mixtures. The opposite effects of CH_3Br on ethane and methane ignitions could be interpreted in terms of these different cycles.

For combustion, the effects of additives are generally divided into two types: chemical and physical effects. With respect to the addition of halogen-containing compounds (RX), the former is predominant.[1]

Most RX's decrease the burning velocity when they are added into a flame.[2] Namely, an RX acts as an inhibitor for flame propagation. Rosser et al.[2] and Westbrook[3] have reported that halogen acid (HX) generated by the decomposition of RX captures H atoms in a flame through the following reaction:

$$HX + H = H_2 + X. \quad (X5)$$

Reaction (X5) is competitive with reaction (R76), which is the most important chain-branching reaction in combustion:

$$H + O_2 = OH + O. \quad (R76)$$

However, the addition effect of RX on ignition is not always similar to that on flame propagation. In previous work,[4-6] we have shown that methyl halides (CH_3X) act as promotors for methane ignition, and discussed the promotion effect on the basis of chemical kinetics.

In this study, in order to examine the addition effect of CH_3X on ethane ignition, the ignition delay times were measured in C_2H_6–O_2–CH_3X mixtures by using a shock tube. Moreover, by means of computational analyses, the chain cycle formed in a C_2H_6–O_2–CH_3Br mixture was compared with that in a CH_4–O_2–CH_3Br mixture.

Experimental

All of the experiments were carried out behind reflected shock waves in a 6.2 cm i.d. stainless steel shock tube. The driver and test sections were 1.7 and 3.8 m long, respectively, so that dwell times above 1.5 ms could be obtained in all of the experiments. Other apparatus for measurements of the shock velocity and ignition delay time and associated procedures have already been reported.[4] Ignition delay times, defined as the time interval between the arrival of a shock wave and the onset of ignition, were obtained by rapid increases in pressure and OH emission ($X^2\Pi_i \leftarrow A^2\Sigma^+$ transition, 306.4 nm).

The compositions of test gas mixtures used are shown in Table 1. The accuracy of the composition of mixtures is better than 0.01%. The measurements were carried out over the temperature range 1200—1900 K and the pressure range 1.4—2.9 atm.

Analytical Treatment

To clarify the addition effects of CH_3X from the viewpoint of the reaction mechanism, ignition delay times were calculated in mixtures 1 (C_2H_6–O_2) and 3 (C_2H_6–O_2–CH_3Br), and sensitivity analyses were carried out. Details concerning the calculation were described previously.[5] The reaction mechanism assembled for ethane oxidation consists of the 93 elementary reactions employed in a previous study on methane oxidation (reactions (R1)—(R93)),[5,6] and 18 reactions added in this study (reactions (R94)—(R111) in Table 2). However, with respect to the rate coefficient of reaction (R38),

Table 1. The Composition of Test Gas Mixture (%)

No.	C_2H_6	O_2	Ar	CH_3Cl	CH_3Br	CH_3I
1	1.00	3.50	95.50	—	—	—
2	1.00	3.50	95.40	0.10	—	—
3	1.00	3.50	95.40	—	0.10	—
4	1.00	3.50	95.40	—	—	0.10

Table 2. Reactions Added in This Study

	Reaction	log A	n	E	Ref.
(R94)	$CH_3+OH=CH_2O+H_2$	12.60	0.00	0.00	7
(R95)	$CH_3+M=CH_2+H+M$	16.29	0.00	91.60	8
(R96)	$CH_3O+H=CH_2O+H_2$	13.30	0.00	0.00	9
(R97)	$C_2H_6+O_2=C_2H_5+HO_2$	13.00	0.00	51.00	10
(R98)	$C_2H_5+O=CH_2O+CH_3$	13.00	0.00	0.00	11
(R99)	$C_2H_5+O=CH_3CHO+H$	13.70	0.00	0.00	12
(R100)	$C_2H_5+CH_3=C_3H_8$	13.93	0.00	6.25	13
(R101)	$C_2H_5+C_2H_5=C_4H_{10}$	12.90	0.00	0.00	12
(R102)	$C_2H_5+C_2H_3=C_4H_8$	12.95	0.00	0.00	13
(R103)	$C_2H_4+C_2H_3=C_4H_6+H$	12.00	0.00	7.30	14
(R104)	$C_2H_3+CH_3=C_3H_6$	13.20	0.00	−4.08	13
(R105)	$C_2H_3+C_2H_3=C_4H_6$	12.95	0.00	0.00	13
(R106)	$C_2H_2+C_2H_2=C_4H_3+H$	13.00	0.00	45.00	15
(R107)	$C_2H_2+C_2H=C_4H_2+H$	13.60	0.00	0.00	15
(R108)	$C_4H_3+M=C_4H_2+H+M$	16.00	0.00	60.00	15
(R109)	$C_4H_2+M=C_4H+H+M$	17.54	0.00	80.00	15
(R110)	$OH+O+M=HO_2+M$	17.00	0.00	0.00	16
(R111)	$H_2O_2+H=H_2O+OH$	14.50	0.00	8.94	17

Rate constants in the form $k=AT^n\exp(-E/RT)$, in cm³, mol, s, kcal, and K units.

Table 3. Reactions Involving Br-Containing Species

	Reaction	log A	n	E	Ref.
(B1)	$CH_3Br=CH_3+Br$	13.20	0.00	71.70	5
(B2)	$CH_3Br+H=CH_3+HBr$	14.24	0.00	6.90	3
(B3)	$CH_3Br+Br=CH_3+Br_2$	13.70	0.00	22.90	3
(B4)	$Br+CH_4=CH_3+HBr$	14.00	0.00	18.30	3
(B5)	$HBr+H=H_2+Br$	11.88	0.50	1.11	3
(B6)	$Br_2+H=HBr+Br$	12.81	0.50	1.11	3
(B7)	$Br+Br+M=Br_2+M$	16.00	0.00	0.00	3
(B8)	$Br+H+M=HBr+M$	18.00	−0.71	0.00	3
(B9)	$Br+C_2H_6=C_2H_5+HBr$	13.90	0.00	13.40	3

Rate constants in the form $k=AT^n\exp(-E/RT)$, in cm³, mol, s, kcal, and K units.

$$C_2H_5\ (+\ M) = C_2H_4 + H\ (+\ M), \qquad \text{(R38)}$$

an expression given by Warnatz,[18]

$$k_{(R38)}(\text{1st order})/s^{-1}$$

$$= 2.00 \times 10^{14}\exp(-39.67\ \text{kcal mol}^{-1}/RT),$$

was employed in this study instead of the expression in the previous one:

$$k_{(R38)}(\text{2nd order})/\text{mol}^{-1}\,\text{cm}^3\,\text{s}^{-1}$$

$$= 2.00 \times 10^{15}\exp(-30.00\ \text{kcal mol}^{-1}/RT).^{19}$$

To complete the reaction model in the presence of CH_3Br, 9 reactions (Table 3) involving Br-containing species (CH_3Br, Br, Br_2, and HBr) were added to the reactions for ethane oxidation. For a comparison, the ignition delay times in CH_4–O_2 and CH_4–O_2–CH_3Br mixtures were also calculated using the same reaction model.

The reverse rate constants were computed using the forward rate constants and the appropriate equilibrium constants. Most thermochemical and thermodynamic data were taken from Refs. 20 and 21. The data for eight species (C_2H_3, C_2H_5, C_2H_6, CH_3O, CHCO, CH_2CO, H_2O_2, and CH_3Br) were not available, and so were evaluated by a statistical method.[20] Details concerning the calculation procedure and the validity of results were descrived previously.[5]

Three methods were carried out to define calculated ignition delay times. The first of these is the time at which the OH concentration increases rapidly, and the second is the time at which C_2H_6 concentration decreases rapidly. The third is the time at which the gas temperature rises rapidly. All of these times agreed to within 7%. Finally, the calculated ignition delay times were determined from the temperature profile, since the error in reading was least.

Results and Discussion

The ignition delay time (τ) measured in mixtures 1—4 are shown in Fig. 1. The addition of CH_3X lengthens τ, i.e., CH_3X inhibits ethane ignition. This

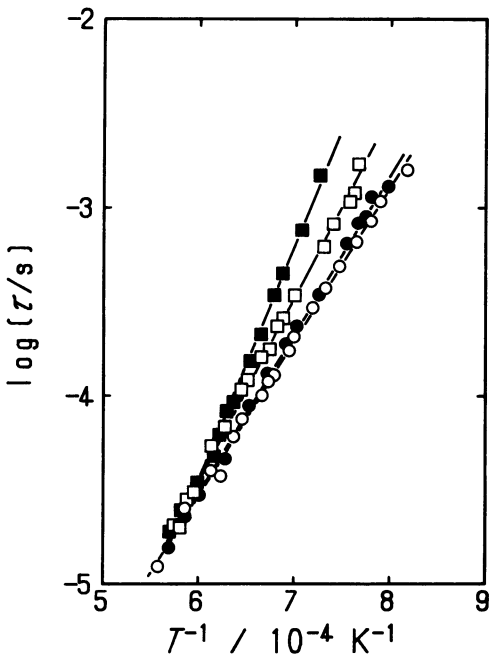

Fig. 1. Measured ignition delay times. ○, Mixture 1; ●, Mixture 2; □, Mixture 3; ■, Mixture 4.

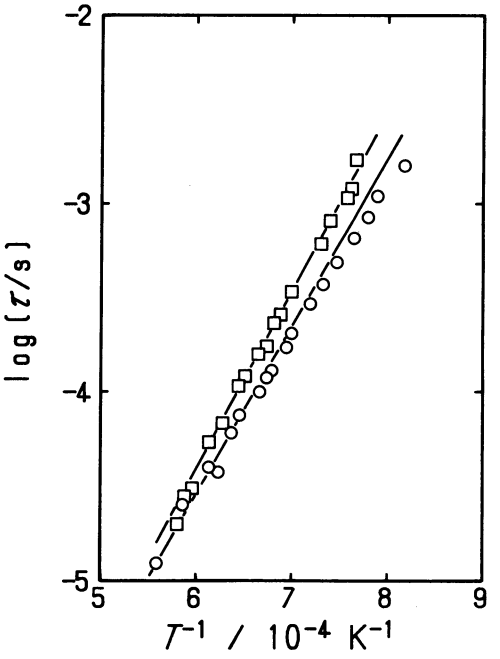

Fig. 2. Comparison between calculated and measured ignition delay times. ○, Mixture 1; □, Mixture 3. Straight lines are calculated.

is contrary to the previous results in which CH_3X promoted methane ignition.[5,6] In three CH_3X compounds (CH_3Cl, CH_3Br, and CH_3I), the inhibition effect of CH_3I is the greatest, while that of CH_3Cl is the least. For all mixtures, plots of $\log \tau$ against the reciprocal of the temperature give straight lines. The slope of the line is 0.81 for mixture 1, while the slopes are 0.85, 0.98, and 1.24 for mixtures 2—4, respectively.

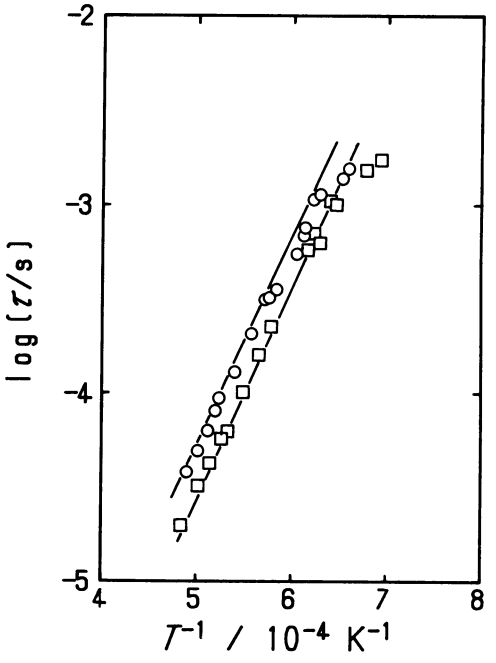

Fig. 3. Comparison between calculated and measured ignition delay times. ○, CH_4–O_2 mixture; □, CH_4–O_2–CH_3Br mixture.[5] Straight lines are calculated.

These values indicate that the inhibition effect of CH_3X is remarkable at low temperature.

In Fig. 2, the ignition delay times calculated in mixtures 1 and 3 are compared with the measured ones. Although the temperature dependence of the calculated values in mixture 1 is somewhat large, the calculated ignition delay times are generally in good agreement with the measured values.

Using the same reaction model, the ignition delay times calculated in CH_4–O_2 and CH_4–O_2–CH_3Br mixtures are shown in Fig. 3. Plots in the figure express the measured values which have already been reported.[5] The ignition delay times re-calculated in this study are identical to those found in the previous one, which were calculated by using 93 reactions for methane oxidation and 8 reactions involving Br-containing species.[5] This agreement indicates that the reactions added in this study (Table 2) have no effect for methane ignition.

As is obvious from Figs. 2 and 3, the assembled reaction mechanism can express the experimental results that CH_3Br promotes methane ignition, but inhibits ethane ignition. To clarify the opposite addition effects of CH_3Br on methane and ethane ignitions, sensitivity analyses were performed on 9 reactions involving Br-containing species (Table 3). In a CH_4–O_2–CH_3Br mixture, the ignition delay times calculated by deleting reactions (B1)—(B9), one by one, are shown in Table 4 (1500 K). Similarly, the ignition delay times calculated at 1500 and 1900 K in mixture 3 (C_2H_6–O_2–CH_3Br) are also shown in Table 4.

Table 4. Calculated Ignition Delay Times

Reaction[a]	Ignition delay time/μs		
	CH_4-O_2-CH_3Br	C_2H_6-O_2-CH_3Br	
	1900 K	1500 K	1900 K
None	56.9	161	8.03
(B1) $CH_3Br=CH_3+Br$	119 (+109%)[b]	163 (+1%)	8.35 (+4%)
(B2) $CH_3Br+H=CH_3+HBr$	74.9 (+32%)	107 (−34%)	6.85 (−15%)
(B3) $CH_3Br+Br=CH_3+Br_2$	57.6 (+1%)	161 (0%)	8.09 (+1%)
(B4) $Br+CH_4=CH_3+HBr$	69.5 (+22%)	163 (+2%)	8.01 (0%)
(B5) $HBr+H=H_2+Br$	54.9 (−4%)	139 (−14%)	7.76 (−3%)
(B6) $Br_2+H=HBr+Br$	56.7 (0%)	160 (0%)	8.01 (0%)
(B7) $Br+Br+M=Br_2+M$	56.7 (0%)	160 (0%)	8.09 (+1%)
(B8) $Br+H+M=HBr+M$	57.2 (+1%)	161 (0%)	8.09 (+1%)
(B9) $Br+C_2H_6=C_2H_5+HBr$	57.7 (+1%)	166 (+3%)	8.15 (+1%)

Calculated ignition dely time is 110 μs at 1900 K in CH_4-O_2 mixture; it is 105 μs at 1500 K and 6.69 μs at 1900 K in C_2H_6-O_2 mixture. a) Reaction which is deleted from the complete mechanism. b) Percentage of change to ignition delay time calculated by using complete mechanism.

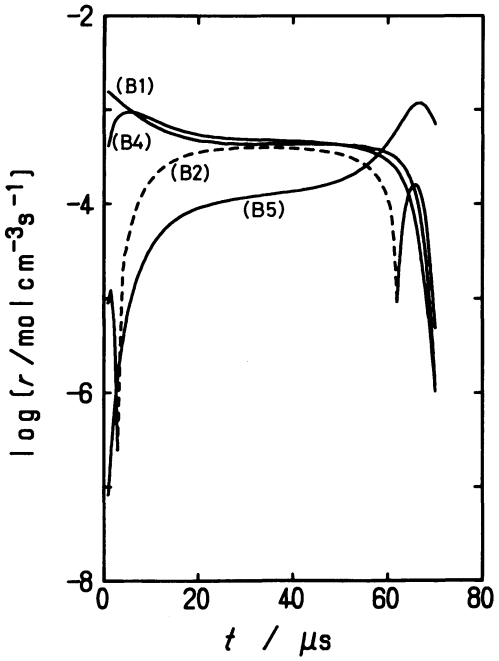

Fig. 4. Net reaction rates of (B1), (B2), (B4), and (B5) at 1900 K in CH_4-O_2 mixture. Calculated ignition delay time is 56.9 μs. t means time after the arrival of reflected shock wave. Solid line: net reaction proceeds in forward direction, dashed line: in reverse direction.

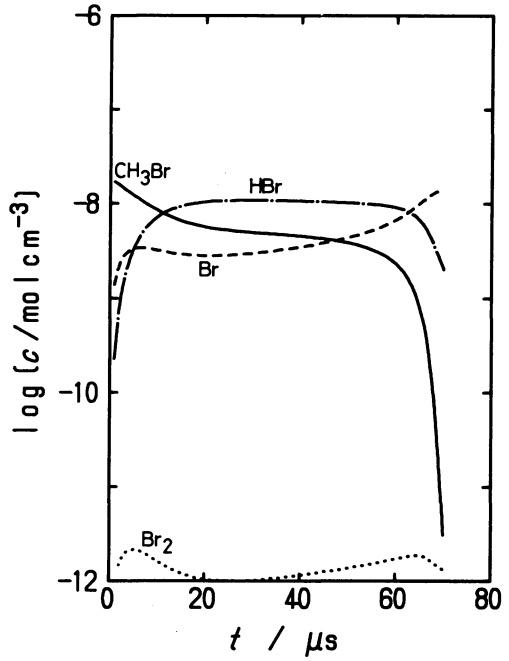

Fig. 5. Calculated concentration profiles of CH_3Br, Br, Br_2, and HBr at 1900 K in CH_4-O_2 mixture.

In a CH_4-O_2-CH_3Br mixture, reactions (B1), (B2), and (B4) greatly influence the ignition delay time (Table 4). When each of these reactions is deleted from the complete mechanism, the ignition delay time is longer than that in the complete mechanism, showing that reactions (B1), (B2), and (B4) promote methane ignition. Moreover, considering the reaction rates (Fig. 4) and the concentrations of Br-containing species (Fig. 5), we arrived at the same conclusion as in a previous study.[5] The following cycle is formed among CH_3Br, Br, and HBr:

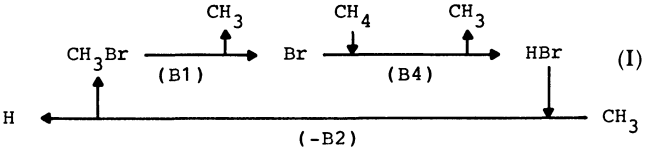

The net reaction of cycle (I) corresponds to the production of one H atom and one CH_3 radical from methane in each chain, and so methane ignition is promoted.

In mixture 3 (C_2H_6-O_2-CH_3Br), the inhibition effect of CH_3Br is remarkable at low temperature, as has been mentioned. From the calculated results at low

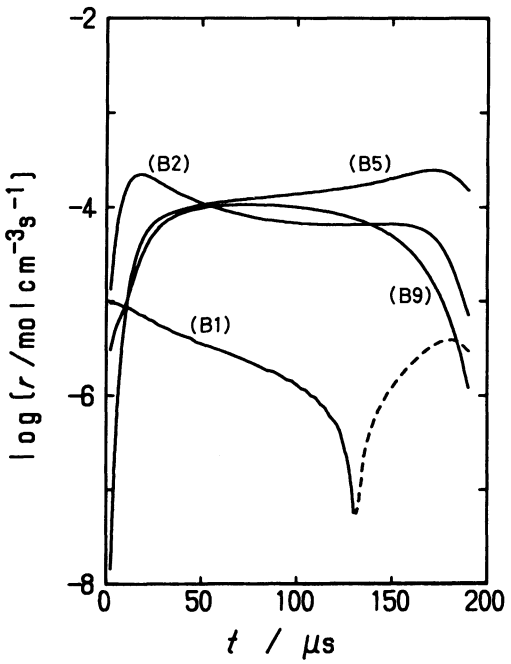

Fig. 6. Net reaction rates of (B1), (B2), (B5), and (B9) at 1500 K in Mixture 3 (C_2H_6-O_2). Calculated ignition delay time is 161 μs.

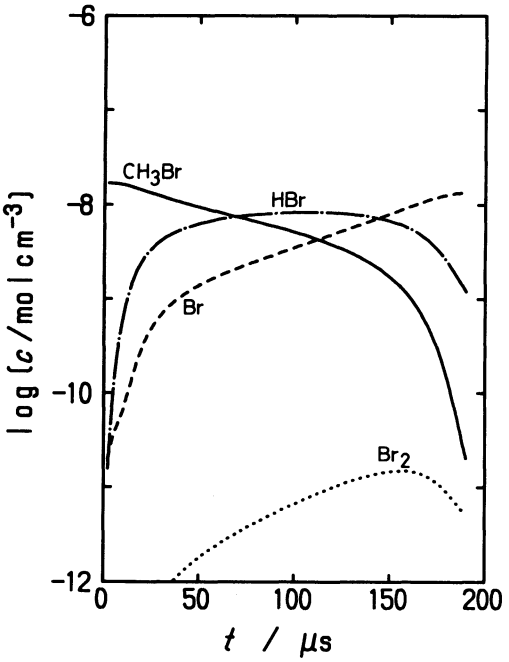

Fig. 7. Calculated concentration profiles of CH_3Br, Br, Br_2, and HBr at 1500 K in Mixture 3 (C_2H_6-O_2).

temperature (1500 K), as shown in Table 4, it is obvious that reactions (B2) and (B5) greatly influence the ignition delay time. Both reactions (B2) and (B5) inhibit ethane ignition, because deletion of these reactions makes the ignition delay time shorter. As shown in Fig. 6, the main reaction of CH_3Br consumption at low temperature is not (B1) but, rather, (B2). Reaction (B2) shows a inhibition effect, because the H atom which is the reactant of the most important chain-branching reaction (R76) controlling ignition is simultaneously consumed. Since the product HBr also mainly reacts with the H atom through reaction (B5), ethane ignition is more inhibited. The bromine atoms consume ethane through reaction (B9), and HBr is regenerated. Reaction (B9), itself, seems to show a promotion effect, because ethane is oxidized through reaction (B9). However, as HBr reproduced through reaction (B9) is the reactant of the inhibition reaction (B5), the promotion effect of reaction (B9) is compensated, as shown in Table 4. This consideration suggests that the following cycle is formed at low temperature in a C_2H_6-O_2-CH_3Br mixture:

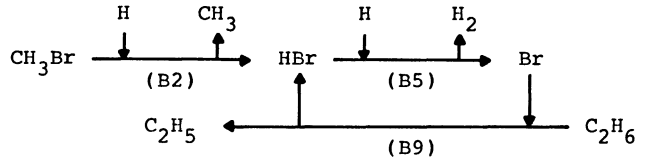

(II)

The difference between the chain cycle formed in the CH_4-O_2-CH_3Br mixture (I) and that in the C_2H_6-O_2-CH_3Br mixture (II) can also be confirmed in the concentration profiles (Figs. 5 and 7). A bromine atom appears earlier than HBr in the CH_4-O_2-CH_3Br mixture, while HBr appears earlier than Br in the C_2H_6-O_2-CH_3Br mixture.

At high temperature, where the inhibition effect of CH_3Br falls, the other channel of CH_3Br consumption, reaction (B1), is open in the C_2H_6-O_2-CH_3Br mixture. As is obvious in Table 4, the inhibition effects due to reactions (B2) and (B5) decrease at high temperature (1900 K). Instead, reaction (B1) shows a slight promotion effect. These reaction rate profiles at 1900 K are shown in Fig. 8. The rate ratio of reaction (B1) to (B2) at the half time of the induction period, $[r(B1)/r(B2)]_{\tau/2}$, is 0.027 at 1500 K, but 0.25 at 1900 K. The increase in the relative rate of reaction (B1) to (B2) is caused by a difference in activation energy between these reactions. Therefore, the cycle formed at high temperature in the C_2H_6-O_2-CH_3Br mixture is expressed as follows.

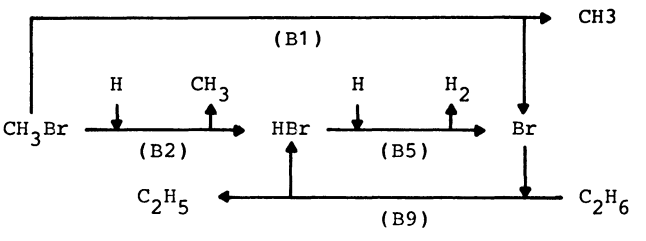

(III)

Reaction (B1), which is competitive with reaction (B2) for CH_3Br consumption, shows a promotion

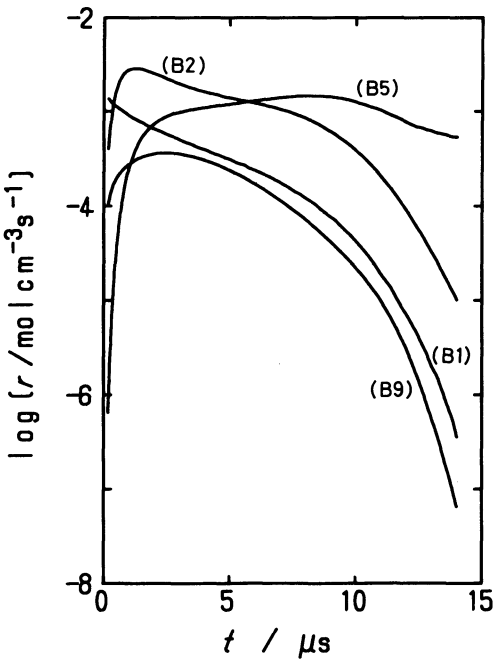

Fig. 8. Net reaction rates of (B1), (B2), (B5), and (B9) at 1900 K in Mixture 3 (C_2H_6–O_2). Calculated ignition delay time is 8.03 μs.

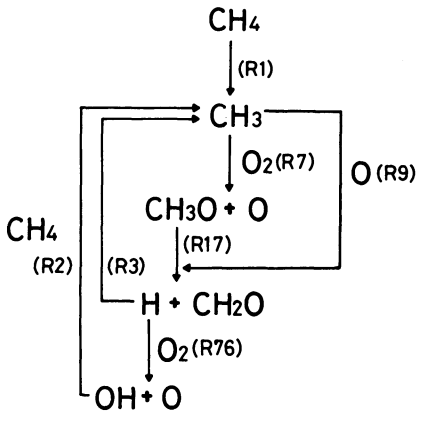

$CH_4 + M = CH_3 + H + M$ (R1)
$CH_3 + O_2 = CH_3O + O$ (R7)
$CH_3O + M = CH_2O + H + M$ (R17)
$CH_3 + O = CH_2O + H$ (R9)
$H + O_2 = OH + O$ (R76)
$CH_4 + OH = CH_3 + H_2O$ (R2)
$CH_4 + H = CH_3 + H_2$ (R3)

Fig. 9. Main process for CH_4 consumption at the early stage of induction period in CH_4–O_2 mixture (1750 K).

effect rather than an inhibition type, as shown in Table 4. The CH_3 radical produced through reaction (B1) accelerates ethane consumption through the path (Fig. 10). Moreover, the relative rates of reactions (B2) and (B5) to the chain-branching reaction (R76) are reduced with temperature, because of the difference in the activation energy between these reactions. The ratios, $[r(B2)/r(R76)]_{\tau/2}$ and $[r(B5)/r(R76)]_{\tau/2}$, are 0.20 and 0.34 at 1500 K, while they are 0.14 and 0.093 at

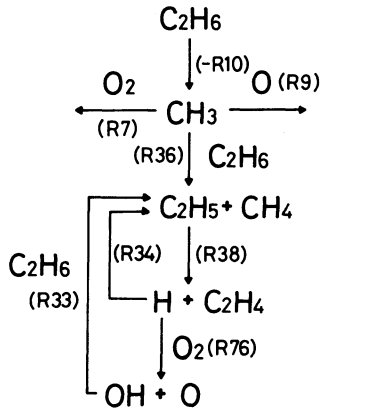

$C_2H_6 = CH_3 + CH_3$ (-R10)
$CH_3 + O_2 = CH_3O + O$ (R7)
$CH_3 + O = CH_2O + H$ (R9)
$C_2H_6 + CH_3 = C_2H_5 + CH_4$ (R36)
$C_2H_5 = C_2H_4 + H$ (R38)
$H + O_2 = OH + O$ (R76)
$C_2H_6 + OH = C_2H_5 + H_2O$ (R33)
$C_2H_6 + H = C_2H_5 + H_2$ (R34)

Fig. 10. Main process for C_2H_6 consumption at the early stage of induction period in Mixture 1 (C_2H_6–O_2, 1750 K).

1900 K. Therefore, it is concluded that competitive reactions (B1) and (R76) with inhibition reactions (B2) and (B5) lower the inhibition effect at high temperature.

In order to consider why the cycle for Br-containing species in the C_2H_6–O_2–CH_3Br mixture differs from that in the CH_4–O_2–CH_3Br mixture, the reaction rates in two CH_3Br-free mixtures were calculated at 1750 K. The main processes for methane and ethane consumption in the early stage of the induction period are summarized in Figs. 9 and 10. The initiation reaction is reaction (R1) for methane oxidation, while it is reaction (−R10) for ethane oxidation. Although both reactions involve a thermal decomposition of fuels, the initial rate of reaction (−R10) is about 2000-times (1750 K) as fast as that of reaction (R1), because of the difference in the dissociation energy. Then, chain cycles, such as shown in Figs. 9 and 10, are formed while consuming methane or ethane.

In these cycles the difference between the consuming rate of CH_3 and that of C_2H_5 is very important. The C_2H_5 radical is mainly consumed through thermal decomposition (R38), while the CH_3 radical is consumed by being reacted with O_2 (R7) or O atoms (R9). The rate coefficient of reaction (R7) is very small. Although the rate coefficient of reaction (R9) is sufficiently large, its reaction rate is not fast, since few O atoms of the reactant exist during the early stage. The rate ratios of reactions (R7) and (R9) in the CH_4–O_2 mxture to reaction (R38) in the C_2H_6–O_2 mixture at 10% of the time of induction period, $[r(R7)_{Me}/r(R38)_{Et}]_{\tau/10}$ and $[r(R9)_{Me}/r(R38)_{Et}]_{\tau/10}$, are 7.5×10^{-4} and 2.6×10^{-4} at 1750 K, respectively. Therefore, the consuming rate of the CH_3 radical is

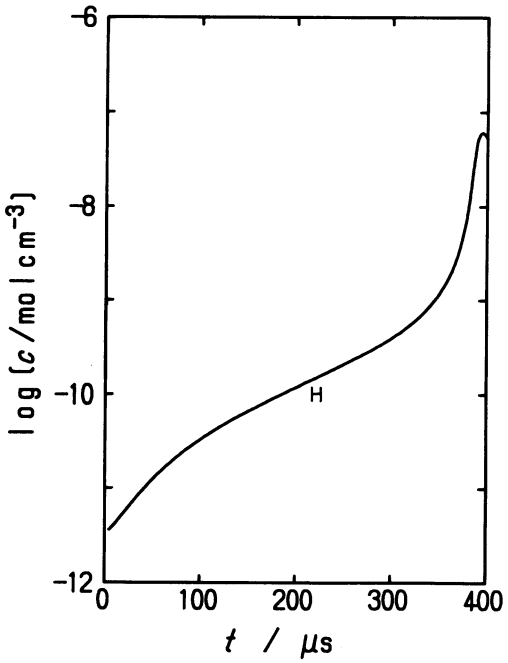

Fig. 11. Calculated concentration profile of H at 1750 K in CH_4–O_2 mixture. Calculated ignition delay time is 360 μs.

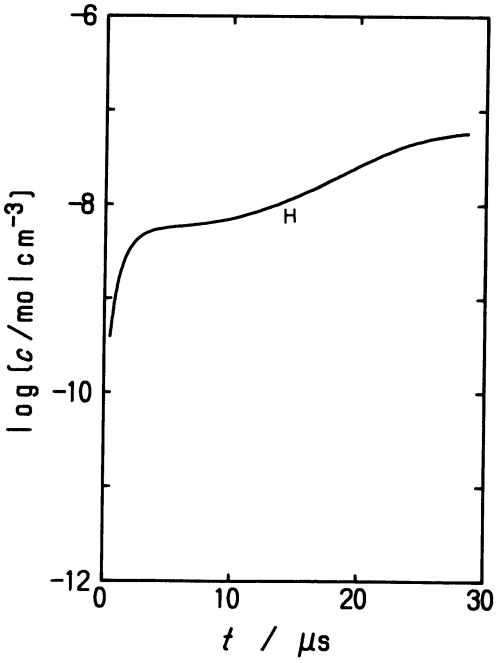

Fig. 12. Calculated concentration profile of H at 1750 K in Mixture 1 (C_2H_6–O_2). Calculated ignition delay time is 16.4 μs.

slower than that of the C_2H_5 radical. This causes a low H concentration during the induction period, as can be seen from a comparison between Figs. 11 and 12. The ratio of the H concentration in the CH_4–O_2 mxture to that in the C_2H_6–O_2 mixture at one half of the induction period, $[[H]_{Me}/[H]_{Et}]_{\tau/2}$, is 0.015 at 1750 K.

From this consideration, we can interpret the opposite effects of CH_3Br on ethane and methane ignitions. With respect to ethane oxidation, since the H concentration is higher during the induction period, reactions (B2) and (B5) are predominant instead of reactions (B1) and (−B2), resulting in an inhibition effect.

The ignition delay times in mixtures 2(C_2H_6–O_2–CH_3Cl) and 4(C_2H_6–O_2–CH_3I) were also calculated using reactions involving Cl- or I-containing species. When the reaction mechanism and the rate coefficients which we had previously used for methane ignition[5,6] were employed, the calculated ignition delay times disagreed with the observed values in both mixtures 2 and 4. The calculation overestimates the ignition delay times in mixture 2, but underestimates them in mixture 4. These disagreements indicate that the assumed reaction mechanism and/or the rate coefficients are impertinent. Thus, more research needs to be carried out in the future.

References

1) K. Akita, *J. Inst. Safty High Pressure Gas Eng.*, **15**, 151 (1978).

2) W. A. Rosser, H. Wise, and J. Miller, "Seventh Symposium (International) on Combustion," The Combustion Institute, Pittsburgh (1958), p. 175.

3) C. K. Westbrook, "Nineteenth Symposium (International) on Combustion," The Combustion Institute, Pittsburgh (1982), p. 127.

4) T. Inomata, T. Moriwaki, and S. Okazaki, *Combust. Flame*, **62**, 183 (1985).

5) K. Takahashi, T. Inomata, T. Moriwaki, and S. Okazaki, *Bull. Chem. Soc. Jpn.*, **61**, 3307 (1988).

6) K. Takahashi, T. Inomata, T. Moriwaki, and S. Okazaki, *Bull. Chem. Soc. Jpn.*, in press.

7) C. P. Fenimore, "Twelfth Symposium (International) on Combustion," The Combustion Institute, Pittsburgh (1969), p. 463.

8) P. Roth, U. Barner, and R. Lohr, *Ber. Bunsenges. Phys. Chem.*, **83**, 929 (1979).

9) K. Hoyermann, N. S. Loftfield, R. Sievert, and H. Gg. Wagner, "Eighteenth Symposium (International) on Combustion," The Combustion Institute, Pittsburgh (1981), p. 831.

10) J. E. Taylor and D. M. Kulich, *Int. J. Chem. Kinet.*, **5**, 455 (1973).

11) K. Hoyermann and R. Sievert, "Seventeenth Symposium (International) on Combustion," The Combustion Institute, Pittsburgh (1979), p. 517.

12) J. Warnatz, "Eighteenth Symposium (International) on Combustion," The Combustion Institute, Pittsburgh (1981), p. 369.

13) C. K. Westbrook and F. L. Dryer, *Prog. Energy Combust. Sci.*, **10**, 1 (1984).

14) S. W. Benson G. R. Haugen, *J. Phys. Chem.*, **71**, 1735 (1967).

15) T. Tanzawa and W. C. Gardiner, Jr., "Seventeenth Symposium (International) on Combustion," The Combustion Institute, Pittsburgh (1979), p. 563.

16) G. S. Bahn, *Pyrodynamics*, **2**, 315 (1965).

17) D. L. Baulch, D. D. Drysdale, and A. C. Lloyd, "High Temperature Reaction Rate Data," Report No. 3, Leeds University, Leeds (1969).
18) Warnats, *Combust. Sci. Tech.*, **34**, 177 (1983).
19) D. B. Olson, T. Tanzawa, and W. C. Gardiner, Jr., *Int. J. Chem. Kinet.*, **11**, 23 (1979).
20) "JANAF Thermochemical Tables," 2nd ed, NSRDS-NBS 37, ed by D. R. Stull and H. Prophet, National Bureau of Standards, Washington D. C., 1971; and later supplements.
21) G. S. Bohn, NASA-CR-2178, NASA, 1973.